applied sciences

MDPI

Article

On the Kinetic Regimes in the Ozonation of Carbamazepine: The Influence of Ozone Concentration in Water Treatment

Marco Antonio Villagómez-Cuéllar [1], Elisabeth Bilbao-García [1], Unai Duoandicoechea [2] and Natalia Villota [2,*]

[1] Department of Environmental and Chemical Engineering, Bilbao School of Engineering, University of the Basque Country UPV/EHU, 48013 Bilbao, Spain; marco.villagomez@gmail.com (M.A.V.-C.); elisabeth.bilbao@ehu.eus (E.B.-G.)

[2] Department of Environmental and Chemical Engineering, Faculty of Engineering Vitoria-Gasteiz, University of the Basque Country UPV/EHU, Nieves Cano 12, 01006 Vitoria-Gasteiz, Spain; unai.duoandicoechea@ehu.eus

* Correspondence: natalia.villota@ehu.eus; Tel.: +34-945013248

Abstract

The removal of persistent pharmaceutical compounds such as carbamazepine (CBZ) by advanced oxidation processes (AOPs) remains a major challenge in water treatment, particularly in relation to understanding the operating conditions governing reaction kinetics and transformation pathways. In this context, this study aims to evaluate the effect of ozone concentration on the kinetics and mechanistic regimes of CBZ ozonation in aqueous solutions. Ozonation experiments were conducted in an aqueous solution at an initial CBZ concentration of 50.0 mg/L, using inlet ozone concentrations between 1.9 and 58.5 g/m^3 under controlled conditions. CBZ degradation followed apparent pseudo-first-order kinetics under the studied conditions, with the corresponding apparent rate constant increasing linearly with the inlet ozone concentration. At ozone concentrations $\geq$ 15.7 g/m^3, rapid CBZ removal was observed, together with high dissolved ozone levels, accelerated loss of aromaticity, and transient formation of colored oxidation intermediates, which were subsequently degraded. In contrast, low ozone concentrations led to ozone-limited kinetics and slower aromatic breakdown. The pH evolution revealed two distinct kinetic regimes, transitioning from oxidant-limited to reaction-controlled behaviour and stabilizing at pH 4.3. These findings may provide guidelines for optimizing ozone-based treatment processes. The insights gained may be applied to the design, scale-up, and operation of advanced and hybrid oxidation systems.

Keywords: advanced oxidation processes; carbamazepine degradation; hybrid oxidation systems; mechanistic insights; oxidation pathways; ozonation; photocatalysis-related AOPs; reaction kinetics; water remediation

Academic Editor: Alejandro Pérez-Larios

Received: 5 May 2026
Revised: 19 May 2026
Accepted: 26 May 2026
Published: 28 May 2026

1. Introduction

The increasing occurrence of pharmaceutical compounds in aquatic environments has emerged as a major concern in environmental engineering and public health [1,2]. In this context, carbamazepine (CBZ) is widely recognized as a representative contaminant due to its high persistence and ubiquitous presence in diverse aquatic matrices, including surface water, groundwater, and treated effluents [3–5]. Its low bio-degradability and poor removal in conventional treatment systems are mainly attributed to its stable tricyclic aromatic structure [6,7]. Consequently, CBZ is commonly used as a model compound to assess the performance of advanced technologies for the removal of refractory micropollutants [8].

Conventional wastewater treatment systems, primarily based on aerobic biological processes, are not specifically designed to remove such emerging contaminants [9–11]. As a result, CBZ removal efficiencies are typically below 20%, contributing to its persistence and potential environmental risks [12]. Given these limitations, advanced oxidation processes (AOPs) have gained attention as effective alternatives, as they enable the degradation of persistent organic compounds through the generation of highly reactive species such as hydroxyl radicals [13–15]. These species exhibit a high oxidation potential (E° = 2.8 V) and react non-selectively with a wide range of organic compounds, facilitating the breakdown of complex and stable molecular structures.

Ozonation represents one of the most established AOPs for micropollutant removal in aqueous systems [16,17]. Ozone (O_3), with an oxidation potential of 2.07 V, can react via two main pathways: direct selective oxidation and indirect non-selective oxidation through hydroxyl radical formation during its decomposition in water [18–20]. The relative contribution of these mechanisms is strongly influenced by operational parameters, such as pH, dissolved ozone concentration, and the presence of radical promoters or scavengers [21]. Recent advances in oxidation chemistry have provided deeper insight into the role of reactive oxygen species (ROS), particularly hydroxyl radicals, in ozone-based systems. These species are now recognized as key contributors to non-selective oxidation pathways, significantly enhancing the degradation of persistent organic contaminants. Understanding the interplay between molecular ozone reactions and radical-mediated pathways is therefore critical for accurately describing reaction kinetics and optimizing advanced oxidation processes [22].

Recent studies have emphasized the growing importance of ozone-based advanced oxidation processes (O_3-AOPs) as versatile tools for the removal of emerging contaminants in water treatment. In particular, recent work has highlighted the effectiveness of ozonation not only as a standalone process but also in hybrid configurations with biological, catalytic, and photochemical systems, improving overall pollutant degradation, biodegradability, and process sustainability. These studies also underline current challenges related to by-product formation, operational costs, and scale-up [23].

In addition, growing research interest in hybrid ozone-based AOPs combined with nanomaterials or photocatalytic systems has been reported in recent years, showing significant improvements in degradation efficiency and mineralization rates due to synergistic effects between oxidant activation and catalytic surfaces [24,25].

In the case of CBZ, ozonation is characterized by fast reaction kinetics, mainly due to the electron-rich nature of its aromatic system [26]. The initial stage of the reaction typically involves the formation of epoxides, which subsequently evolve through successive oxidation steps into quinones, carbonyl compounds, and ultimately products derived from aromatic ring cleavage [27]. However, although these transformations lead to the removal of the parent compound, complete mineralization is not always achieved, and potentially toxic byproducts may accumulate [28]. Therefore, a combined analysis of degradation kinetics and transformation pathways is essential for a comprehensive assessment of the process [29].

Several studies have reported the high reactivity of CBZ toward ozone, typically describing its degradation by pseudo-first-order kinetics under conditions of ozone excess. For instance, McDowell et al. investigated CBZ ozonation focusing on the identification of transformation products and reaction pathways, confirming rapid oxidation and the formation of epoxide and oxygenated intermediates [21]. Similarly, Broséus et al. evaluated the removal of various pharmaceuticals, including CBZ, during ozonation in drinking water treatment, reporting high removal efficiencies but providing limited insight into the influence of ozone dosage on kinetic regimes [26].

Despite these contributions, previous studies have primarily focused on degradation efficiency or product identification under fixed conditions, with limited emphasis on how variations in ozone concentration influence kinetic regime transitions. In particular, the role of ozone concentration as a governing parameter linking oxidant availability, kinetic behaviour, and transformation pathways remains insufficiently explored.

In contrast, the present work systematically investigates CBZ ozonation over a wide range of inlet ozone concentrations (1.9–58.5 g/m^3), enabling the identification of distinct kinetic regimes and the quantitative establishment of a linear relationship between ozone concentration and apparent reaction rate. This approach provides a mechanistic framework that goes beyond conventional pseudo-first-order descriptions and allows direct comparison between ozone-limited and oxidant-saturated conditions, which has not been comprehensively addressed in previous studies.

From a kinetic perspective, CBZ degradation by ozonation is often described using pseudo-first-order models under conditions of excess ozone [30]. However, this simplified approach may not adequately represent real systems, where mass transfer limitations and parallel reactions can occur [31]. In gas–liquid systems, ozone must first dissolve into the aqueous phase before reacting with contaminants, which may limit the overall reaction rate, particularly under conditions of low ozone partial pressure or insufficient mixing [32].

The interplay between mass transfer and chemical kinetics leads to the existence of different operational regimes [33]. In an ozone-limited regime, the degradation rate is directly governed by the availability of dissolved ozone and the mass transfer rate. In contrast, in a reaction-controlled regime, ozone is present in excess, and the rate depends solely on intrinsic reaction kinetics [34]. Identifying the transition between these regimes is crucial for process optimization, as it directly impacts ozone consumption, reactor design, and overall treatment efficiency [35].

Despite its importance, there is still a lack of systematic studies addressing the influence of ozone concentration on CBZ degradation kinetics [36]. Most existing works focus primarily on removal efficiencies or byproduct identification, with limited attention to the relationship between ozone dosage, kinetic regime shifts, and mass transfer constraints [37]. Furthermore, variations in physicochemical conditions, including pH changes and the accumulation of intermediate species, can significantly affect both degradation pathways and overall reaction rates [38]. This highlights the need for integrated studies combining kinetic modeling with mass transfer analysis.

In parallel, heterogeneous photocatalysis using nanomaterials has emerged as a promising advanced oxidation process for pollutant degradation [39–42]. These systems rely on the generation of reactive oxygen species under light irradiation, sharing common mechanistic features with ozonation, particularly in terms of oxidative pathways and intermediate formation.

Although ozonation and photocatalysis are often treated as independent processes, they share common fundamental mechanisms [13,40]. Both rely on the generation of highly reactive oxidizing species capable of transforming complex organic molecules into simpler compounds and eventually achieving mineralization. For aromatic compounds such as CBZ, these processes involve initial electrophilic attack on the aromatic ring, followed by the formation of oxygenated intermediates and subsequent ring opening. This shared mechanistic basis provides a bridge between ozonation and nanomaterial-driven photocatalytic systems, reinforcing the relevance of the present study within the context of photocatalysis research.

The integration of ozonation and photocatalysis has led to the development of hybrid processes exhibiting significant synergistic effects [36]. In these systems, ozone can act as an electron acceptor, reducing electron–hole recombination in the photo-catalyst and

enhancing the generation of oxidizing species. Simultaneously, photo-catalytic activity can promote ozone decomposition, increasing hydroxyl radical production and improving overall process efficiency [19]. These synergies underscore the importance of understanding ozone reaction mechanisms as a basis for designing more efficient hybrid systems. Here, the analysis of ozone concentration effects becomes particularly relevant. As in ozonation, photocatalytic processes are also influenced by the balance between mass transfer and reaction kinetics. Thus, identifying kinetic regimes in ozonation systems can provide valuable insights for interpreting photocatalytic behaviour, especially in nanocatalyst-based systems.

Despite the extensive literature on CBZ degradation using advanced oxidation processes, limited attention has been paid to the role of ozone concentration as a governing parameter controlling reaction kinetics and the transition between kinetic regimes. In reactive gas–liquid systems, the coupling between mass transfer and chemical reaction can significantly influence apparent kinetic behaviour, yet this aspect has not been systematically addressed. Understanding these interactions is essential not only for ozonation systems, but also for interpreting and optimizing photocatalytic processes, including those based on nanomaterials, where similar oxidative pathways are involved.

Although this study focuses on ozonation, its scope is closely related to photocatalytic processes based on nanomaterials, as both systems rely on the generation of reactive oxygen species and share common oxidation pathways for the degradation of organic pollutants. In particular, the interplay between oxidant availability, reaction kinetics, and mass transfer identified in this work provides fundamental insight into the mechanisms governing advanced oxidation processes. These factors are also critical in nanomaterial-based photocatalytic systems, where catalyst properties, light absorption, and reactive species generation determine overall performance.

Unlike conventional studies that primarily focus on pollutant removal efficiency or identification of transformation products under fixed operating conditions, the present work specifically addresses the influence of ozone concentration as a governing parameter controlling reaction kinetics, mass transfer behaviour, and the transition between kinetic regimes. By systematically varying ozone concentration over a wide range and combining kinetic analysis with multiple independent physicochemical indicators, this study moves beyond a purely descriptive approach and provides a mechanistic framework for understanding and optimizing ozonation processes in reactive gas–liquid systems.

In this context, this study aims to systematically investigate CBZ ozonation under varying ozone concentrations, with particular emphasis on identifying kinetic regimes and their mechanistic interpretation in a coupled mass transfer–reaction system. By establishing a quantitative relationship between oxidant availability and apparent reaction kinetics, this work provides a coherent framework directly aligned with the scope of the manuscript and relevant for the interpretation and optimization of ozone-based advanced oxidation processes.

The novelty of the present work lies not in the demonstration of CBZ degradation itself, which is well established, but in the systematic identification and interpretation of kinetic regimes governed by oxidant availability in a coupled gas–liquid reactive system. Unlike most previous studies on contaminant–oxidant systems, which are typically conducted under fixed or excess oxidant conditions, this work explicitly demonstrates the transition between ozone-limited and reaction-controlled regimes and establishes a quantitative relationship between ozone concentration and apparent reaction kinetics. Furthermore, by integrating kinetic analysis with independent physicochemical indicators, the study provides a mechanistic framework linking oxidant availability, mass transfer, and transformation pathways, which is transferable to other advanced oxidation processes.

2. Materials and Methods

Carbamazepine (CBZ, purity ≥ 99%) was supplied by Fagron (Rotterdam, The Netherlands) and used without further purification. All aqueous solutions were prepared with distilled water. Hydrochloric acid (HCl, 37%) and sodium hydroxide (NaOH, pellets) were used for pH adjustment. High-purity oxygen (≥99.999%, Air Liquide, Madrid, Spain) was employed as the feed gas for ozone generation. An initial CBZ concentration of 50.0 mg/L was selected for all experiments. This concentration was intentionally chosen to allow precise mechanistic monitoring of ozone consumption, pH evolution, aromaticity loss and formation of transient intermediates, which cannot be reliably detected at environmentally relevant CBZ levels due to analytical limitations. This approach is widely adopted in mechanistic studies of advanced oxidation processes and is not intended to replicate real wastewater concentrations.

Ozonation experiments were carried out in a laboratory-scale semi-continuous reactor with an effective working volume of 1.0 L (Figure 1). The reactor was equipped with four ports allowing the simultaneous insertion of a pH electrode, a dissolved ozone probe, a gas injection line, and a sampling outlet. The solution was continuously stirred at 500 rpm to ensure complete homogenization and minimize mass-transfer limitations. Temperature was maintained at 25 ± 1 °C using an external thermostatic bath (Frigiterm-P, Selecta, Barcelona, Spain) connected to an internal quartz recirculation sleeve. Ozone was generated from pure oxygen using a corona discharge ozone generator (Triogen LAB2B, BIO-UV Group, Lunel, France). The applied gas flow rate was fixed at 1.0 L/min and regulated using a precision control valve.

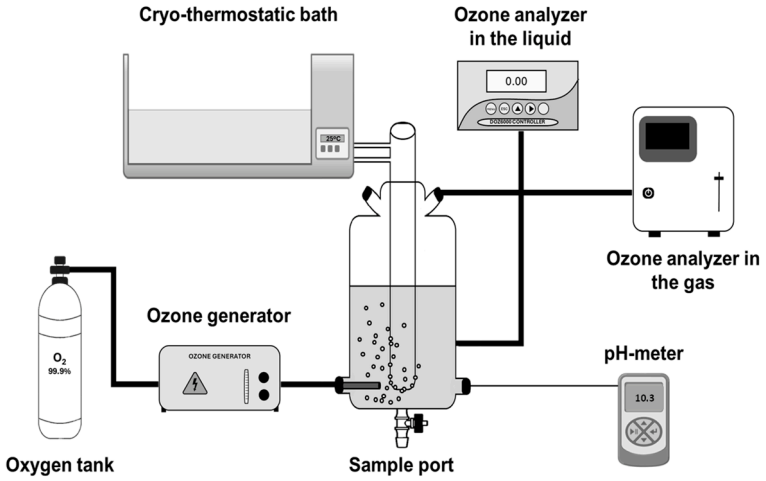

Figure 1. Experimental ozonation setup at laboratory scale.

Ozone was introduced into the liquid phase through a silicon carbide gas injection system (Pawfly ASC 025, Aipade, Shenzhen, China) installed at the bottom of the reactor. The injection device was designed to generate different bubble size distributions: a conventional injector producing small bubbles (diameter ≈ 2 mm) and a micro-diffuser generating micro-bubbles with diameters below 0.5 mm. Excess ozone in the off-gas was destroyed using an ozone destructor prior to venting, ensuring safe operation. All experiments were conducted at a constant initial pH 10, adjusted prior to ozonation using small volumes of concentrated HCl or NaOH to avoid dilution effects. Once adjusted, no further pH control was applied during the reaction, and pH evolution was monitored continuously. The inlet ozone concentration in the gas phase was systematically varied between 1.9 and 58.5 g/m^3 in order to investigate its influence on CBZ degradation kinetics, reaction regimes, ozone accumulation and oxidation pathways. The selected concentration

range spans from ozone-limited to oxidant-saturated conditions, enabling identification of transitions between different kinetic regimes.

Each experimental run was performed using freshly prepared CBZ solutions. Due to the slow dissolution kinetics of CBZ in water, solutions were prepared at least 24 h prior to ozonation to ensure complete solubilization. Control experiments were carried out in the absence of ozone under identical conditions to confirm that no CBZ degradation occurs due to hydrolysis or pH effects alone. All experiments were performed at least in duplicate, and mean values are reported. Deviations observed between experiments were within experimental uncertainty. All experiments were performed at least in duplicate, and deviations between replicates were within the experimental uncertainty, confirming the high reproducibility of the system.

CBZ concentration was quantified by high-performance liquid chromatography (HPLC) using a Waters 2695 system equipped with a dual-wavelength UV detector (Model 2487, Waters, Milford, MA, USA). Separation was achieved using a Zorbax Eclipse PAH column (150 mm × 4.6 mm, 5 µm) with a corresponding guard column. The mobile phase consisted of water and acetonitrile (ACN) at a flow rate of 0.8 mL/min. The gradient program started at 20% ACN, increased linearly to 45% (v/v) in 3 min, was held for 6 min, and then returned to the initial conditions. The total run time was 10 min, with an injection volume of 50.0 µL. CBZ was detected at 275 nm and identified by comparison of retention times with external standards. pH was monitored online using a Hanna Instruments HI2003 electrode. Dissolved ozone concentration was measured continuously with a DOZ6000 dissolved ozone probe (Chemtrac Inc., Norcross, GA, USA), while ozone concentration in the gas phase was determined using a BMT 964C ozone analyzer (Ozone Solutions Inc., Hull, IA, USA). Aromaticity changes were monitored by UV–Vis spectrophotometry (Jasco V-630, Madrid, Spain) through absorbance measurements at 254 nm, whereas colour development was quantified at 455 nm. Turbidity was measured using a nephelometric turbidimeter (HI88703, Hanna Instruments, Eibar, Spain) according to ISO 7027 [43] and USEPA Method 180.1, and reported in NTU.

The initial CBZ concentration employed in this study (50.0 mg/L) is significantly higher than typical levels found in real wastewater systems, where concentrations are usually in the µg/L range. This elevated concentration was intentionally selected to facilitate a detailed mechanistic analysis, enabling accurate monitoring of ozone consumption, reaction kinetics, pH evolution, and the formation and decay of intermediate species, which are often difficult to detect at environmentally relevant concentrations due to analytical limitations. Such an approach is commonly adopted in mechanistic studies of advanced oxidation processes, where higher pollutant concentrations are used to improve analytical resolution and kinetic interpretation [13,20].

Although absolute degradation rates and reaction times may differ under real conditions, the fundamental mechanisms governing CBZ ozonation, including the role of ozone concentration, the transition between ozone-limited and reaction-controlled regimes, and the formation of transient oxidation intermediates, are not expected to change significantly at lower concentrations. Instead, these results provide intrinsic kinetic and mechanistic insights that are transferable to real systems after appropriate scaling and consideration of matrix effects.

In practical wastewater treatment scenarios, additional factors such as the presence of natural organic matter, radical scavengers, and inorganic constituents may influence ozone consumption and reduce process efficiency. Therefore, the kinetic relationships and regime-based interpretation developed in this work should be understood as a reference framework that can support the design and optimization of ozonation and hybrid advanced oxidation processes under real operating conditions.

It should be noted that, although the application of multiple independent kinetic methods (e.g., initial rates or integral approaches) is commonly recommended for homogeneous systems, their direct use in the present study is limited by the nature of the ozonation process. In this gas–liquid system, ozone concentration in the aqueous phase is not constant but results from the dynamic coupling of mass transfer and fast chemical reaction. Therefore, the assumptions required for classical kinetic methods are not fulfilled. Instead, the kinetic analysis was performed using an apparent pseudo-first-order approach, which provides a practical and physically consistent framework for describing pollutant degradation under non-constant oxidant conditions. The validity of this approach is supported by the consistent trends observed across multiple independent experimental indicators, including CBZ concentration decay, dissolved ozone profiles, pH evolution, and spectroscopic measurements (UV_{254} and colour), all of which converge toward the identification of distinct kinetic regimes governed by ozone availability.

3. Results

3.1. Kinetics of Carbamazepine Ozonation in Water

The kinetic behaviour of carbamazepine (CBZ) during ozonation was systematically investigated by varying the inlet ozone concentration, covering a wide range of conditions from ozone-limited to oxidant-saturated regimes. Figure 2 illustrates the temporal evolution of CBZ concentration at different ozone dosages, while temperature 25 °C and initial pH 10.3 were kept constant. Each data point represents the experimentally determined concentration of carbamazepine (CBZ) at a given reaction time, while the legend specifies the inlet ozone concentration associated with each experimental condition. The solid black lines shown in Figure 2 correspond to the analytical solution of the apparent pseudo-first-order kinetic model described by Equations (1)–(3).

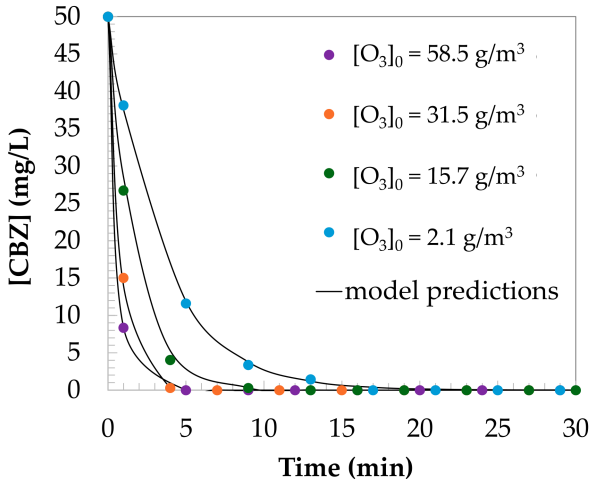

Figure 2. Kinetic degradation of CBZ during ozonation treatment. Experimental conditions: $[CBZ]_0$ = 50.0 mg/L; [T] = 25 °C; $[pH]_0$ = 10.3.

The model parameters (k_{CBZ}) were obtained by nonlinear regression of the experimental concentration profiles using a least-squares fitting procedure. This approach allows a quantitative assessment of the agreement between experimental data and model predictions under different ozone concentrations. Under all operating conditions, CBZ degradation proceeds rapidly at the beginning of the process and then gradually slows down as the reaction progresses, indicating a strong dependence of the degradation rate on oxidant availability.

At high inlet ozone concentrations (31.5 and 58.5 g/m^3), CBZ removal is very fast, with nearly complete degradation occurring within the first few minutes of reaction. By

contrast, at lower ozone concentrations (15.7 and especially 2.1 g/m^3), CBZ degradation is considerably slower, and much longer reaction times are required to reach similar levels of removal. These findings highlight the key role of ozone concentration in controlling reaction kinetics and indicate the existence of distinct kinetic regimes governed by oxidant supply. The kinetic trends observed are consistent with the general behaviour of advanced oxidation processes, in which pollutant degradation is primarily governed by the rate of generation of reactive oxygen species.

Based on the kinetic profiles shown in Figure 2, CBZ degradation shows a clear dependence on the applied ozone concentration, revealing well-defined reaction regimes controlled by oxidant availability. The progressively steeper decay curves observed at higher ozone dosages contrast sharply with the slower kinetic response under ozone-limited conditions, highlighting the central role of reactive oxygen species generation in determining overall degradation rates and in driving the transition from oxidant-limited to oxidant-excess regimes. To describe these trends quantitatively and allow for a rigorous comparison between operating conditions, a kinetic model was applied to extract apparent first-order rate constants from the experimental data. The resulting kinetic parameters, summarized in Table 1, establish a quantitative relationship between ozone concentration and reaction rate and define a benchmark for CBZ oxidation under purely chemical ozonation conditions. The inlet ozone concentration is expressed in g/m^3, while the apparent first-order degradation rate constants are reported in 1/min. This benchmark is particularly valuable in the context of nanomaterials-assisted photocatalysis, as it provides a reference against which the added benefits of light activation, catalyst surface effects and enhanced radical generation in photocatalytic and hybrid ozone–photocatalytic systems can be objectively evaluated.

Table 1. Kinetic parameters estimated according to the proposed mathematical model.

$[O_3]_0$ (g/m^3)	k_{CBZ} (1/min)	$[UV_{254,CBZ}]_0$ (AU)	$[UV_{254}]_{final}$ (AU)	k_{Af} (1/min)	k_{Ad} (1/min)
1.9	0.287	1.4	1.013	0.07	0.08
15.7	0.563	1.4	0.292	0.40	0.07
31.5	1.277	1.4	0.468	0.60	0.12
58.5	1.788	1.4	0.530	0.70	0.5

On the basis of the kinetic regimes identified, CBZ degradation during ozonation was described using an apparent first-order kinetic model. This approach enables a straightforward comparison of reaction rates across different ozone concentrations and offers a practical framework for benchmarking oxidant-driven processes against more complex photocatalytic and hybrid advanced oxidation systems. In this work, kinetics are described using an apparent pseudo-first-order model with respect to CBZ concentration, which is appropriate for reactive gas–liquid systems where oxidant concentration is not constant. Accordingly, CBZ degradation was represented by an apparent first-order differential rate expression, as shown in Equation (1).

$$\frac{d\,[CBZ]}{dt} = -k_{CBZ}\,[CBZ] \tag{1}$$

Integration of this expression yields the corresponding first-order kinetic form given by Equations (2) and (3).

$$\int_{[CBZ]_0}^{[CBZ]} \frac{d\,[CBZ]}{[CBZ]} = -k_{CBZ} \int_0^t dt \tag{2}$$

$$[CBZ] = [CBZ]_0 \, exp(-k_{CBZ} \, t) \quad (3)$$

The assumption of apparent pseudo-first-order kinetics is not based solely on visual inspection of concentration profiles. To validate this approach, the experimental data were also analysed using linearized kinetic plots (ln ([CBZ]/[CBZ]$_0$) versus time), which exhibited an approximately linear behaviour over the initial reaction period. This supports the use of a pseudo-first-order approximation under the studied conditions.

Based on the experimental data, an empirical relationship was established between the apparent pseudo-first-order rate constant and the inlet ozone concentration, as expressed in Equation (4). The apparent rate constant integrates both chemical reaction kinetics and ozone transfer effects. This correlation reflects the effect of oxidant availability under the studied operating conditions and should not be interpreted as an intrinsic kinetic rate law. The linear trend observed is consistent with the transition from ozone-limited to oxidant-saturated regimes and captures the combined influence of mass transfer and chemical reaction.

$$k_{CBZ} = 0.0176 \, [O_3]_0 + 0.2357 \quad (4)$$

where

[CBZ]: carbamazepine concentration (mg/L)

[CBZ]$_0$: initial carbamazepine concentration (=50.0 mg/L)

t: time (min)

k$_{CBZ}$: apparent pseudo-first-order rate constant for CBZ degradation (1/min)

It is important to note that Equation (4) does not represent a fundamental kinetic rate law derived from reaction mechanism, but rather an empirical correlation obtained from regression of the apparent rate constants (k$_{CBZ}$) listed in Table 1 as a function of inlet ozone concentration. Therefore, this relationship reflects the combined effect of ozone mass transfer and chemical reaction under the specific experimental conditions of this study.

Finally, the kinetic parameters derived from the ozonation experiments (Figure 2 and Table 1) provide a quantitative basis for interpreting CBZ degradation mechanisms and position chemical ozonation as a reference process for evaluating the performance and added value of nanomaterials-assisted photocatalytic and hybrid advanced oxidation systems.

3.2. Changes in Water pH During CBZ Ozonation

As shown in Figure 3a, the pH of the aqueous medium undergoes significant variations during the ozonation of carbamazepine (CBZ), reflecting the chemical transformations occurring throughout the process. For a proper interpretation of these results, it is essential to consider the ozone injection system employed, as it directly governs gas–liquid mass transfer and, consequently, the availability of oxidants in the aqueous phase.

The conventional diffuser generates relatively large bubbles, resulting in a lower interfacial area per unit volume and, consequently, slower ozone dissolution kinetics. In addition, these bubbles rise rapidly within the reactor, reducing gas–liquid contact time. As a result, the concentration of dissolved ozone remains relatively low, limiting the intensity of oxidative reactions.

In contrast, the use of a micro-diffuser capable of producing much smaller microbubbles significantly increases the gas–liquid interfacial area and prolongs ozone residence time in the liquid phase. This configuration substantially enhances ozone mass transfer efficiency, allowing higher dissolved ozone concentrations to be achieved. Moreover, microbubbles promote ozone decomposition in water, favouring the formation of hydroxyl radicals and enhancing advanced oxidation pathways. Overall, the micro-diffuser enables a more efficient utilization of ozone, whereas the conventional diffuser exhibits limitations associated with poorer mass transfer and lower oxidant availability.

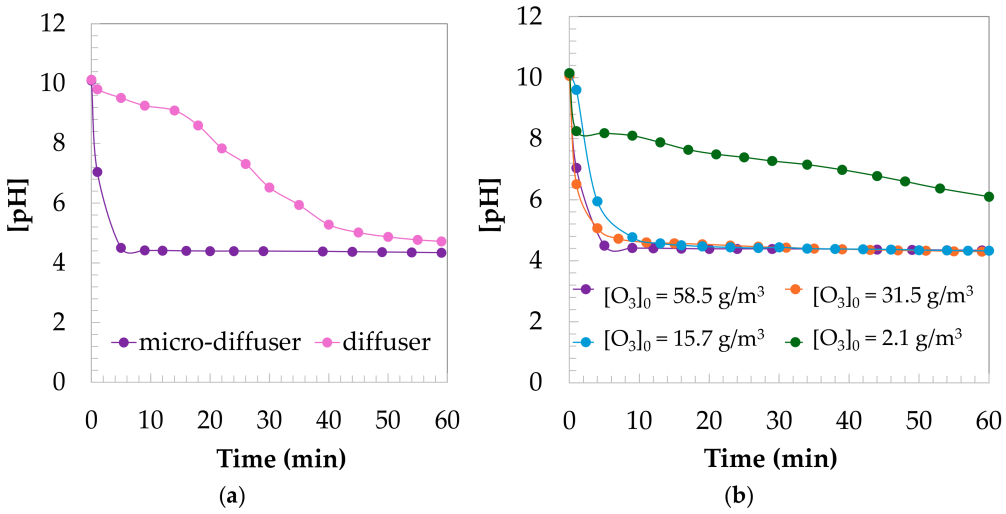

Figure 3. Temporal evolution of pH during CBZ ozonation: (**a**) effect of the ozone gas injection system operating at an ozone dosage of 58.8 g/m^3; (**b**) effect of the injected ozone dosage using a micro-diffuser. Experimental conditions: $[CBZ]_0$ = 50.0 mg/L; [T] = 25 °C; $[pH]_0$ = 10.3.

Under the experimental conditions studied, an initial decrease in pH is observed. This behaviour is attributed to the formation of reactive oxidizing species and acidic intermediate products, primarily carboxylic acids, generated through the reaction of ozone with CBZ as well as its interaction with water. These acidic compounds contribute significantly to the acidification of the medium during the early stages of the ozonation process.

As ozonation proceeds, the organic intermediates formed are progressively mineralized into carbon dioxide and water. This process reduces the concentration of strong acidic organic species; however, it simultaneously releases CO_2, which dissolves in water and equilibrates to form carbonic acid. Consequently, the system evolves toward a pH value governed mainly by the $CO_2/H_2CO_3/HCO_3^-$ equilibrium. Under typical conditions of aqueous CO_2 saturation, this equilibrium stabilizes at a pH close to 4.0. Therefore, even after most organic matter has been degraded, the pH does not return to neutral values but remains around pH 4.0 due to the carbonic acid–bicarbonate buffering system resulting from mineralization.

Accordingly, the pH profiles recorded during CBZ ozonation exhibit a characteristic pattern consisting of an initial sharp decrease followed by a stabilization phase. This behaviour provides indirect evidence of the formation of acidic intermediates and their subsequent mineralization, and it can be considered an indicator of the overall efficiency of the ozonation process.

Regarding the time required to reach pH stabilization, a marked difference is observed depending on the ozone injection system. When ozone is introduced using a micro-diffuser, the initial pH drop is completed within approximately 5 min, whereas the same process extends to nearly 60 min when the conventional diffuser is employed. This difference can be explained by ozone mass transfer efficiency: the micro-diffuser generates much smaller bubbles, substantially increasing the gas–liquid interfacial area and promoting rapid ozone dissolution. As a result, the oxidative reactions responsible for acid formation proceed more intensively and within a significantly shorter time frame. Conversely, the larger bubbles produced by the conventional diffuser exhibit a lower specific surface area, slowing ozone dissolution and extending the time required for the system to reach acidic equilibrium.

Figure 3b shows the pH evolution during CBZ ozonation using the micro-diffuser and different inlet ozone concentrations. At low ozone concentrations, on the order of 1.9 g/m^3, pH decreases slowly and almost linearly, following zero-order kinetics. In contrast, when higher ozone concentrations are applied (15.7–58.5 g/m^3), very similar pH profiles are

observed, independent of the ozone gas flow rate. In these cases, pH rapidly decreases from 10.3 to approximately 4.3 within about 10 min and remains stable at this value for the remainder of the treatment.

This behaviour indicates that above a certain ozone concentration threshold, the rate of medium acidification is no longer limited by oxidant availability but becomes controlled by the degradation kinetics of CBZ and its reaction intermediates. Under high inlet ozone concentrations, CBZ oxidation proceeds rapidly and efficiently, leading to the formation of oxygenated compounds and low-molecular-weight organic acids, such as formic, acetic, or maleic acids, which are responsible for the sharp initial pH decrease. Once pH $\approx$ 4.3 is reached, the system enters a dynamic equilibrium region in which the formation of new organic acids is balanced by their subsequent oxidation, explaining the observed pH stabilization.

By contrast, at very low ozone concentrations, the oxidative process is less intense and the formation of acidic products occurs more gradually, resulting in a slow and nearly linear acidification of the medium. Overall, these observations clearly reveal the existence of two distinct kinetic regimes: at 1.9 g/m^3, an ozone-limited regime characterized by low oxidizing capacity, and at 15.7–58.5 g/m^3, a regime controlled by the rate of organic acid generation and transformation, associated with a high oxidizing capacity of the system.

3.3. Transformation of Organic Matter During CBZ Ozonation

Beyond the disappearance of the parent compound, the ozonation of carbamazepine involves a complex transformation of organic matter, which can be tracked through changes in its structural and optical properties. To gain deeper insight into the oxidation pathways and the nature of intermediate species formed during the process, the evolution of aromaticity, color, and turbidity was systematically monitored. These complementary indicators provide valuable information on the progressive breakdown of aromatic structures, the transient formation and subsequent decay of oxidation by-products, and the aggregation or dispersion phenomena occurring in the aqueous phase during CBZ ozonation.

3.3.1. Oxidative Loss of Aromaticity

During the ozonation of CBZ, the loss of water aromaticity (UV_{254}, Absorbance Units) constitutes a key indicator of the extent of compound degradation. As shown in Figure 4a, the evolution of normalized aromaticity during CBZ ozonation is strongly dependent on the type of ozone diffusion system employed. When a conventional diffuser is used at an ozone dosage of 58.8 g/m^3, water aromaticity initially increases during the first 15 min of treatment and subsequently stabilizes at a nearly constant value. This initial rise in aromaticity can be attributed to the limited ozone mass transfer efficiency associated with the formation of relatively large bubbles, which provide a lower gas–liquid interfacial area and hinder ozone dissolution during the early stages of the process.

Under these conditions, CBZ is not immediately fully degraded; instead, transient aromatic intermediates are formed as a result of partial oxidation reactions, such as hydroxylated derivatives or partially opened but still conjugated aromatic fragments. The accumulation of these intermediates leads to enhanced absorbance in the characteristic aromatic region at 254 nm, producing an apparent increase in aromaticity. Once a dynamic balance is reached between the formation and further degradation of these intermediates, UV absorbance stabilizes over time.

In contrast, when ozone is injected using a micro-diffuser, a progressive decrease in absorbance in the aromatic region is observed, reflecting the effective disruption of the CBZ molecular structure. This behaviour is associated with the high reactivity of ozone, which preferentially attacks the conjugated double bonds within the aromatic ring system,

initiating addition and oxidation reactions that ultimately lead to ring opening. During the initial stages of ozonation, aromatic degradation proceeds rapidly due to the high concentration of dissolved ozone and the inherent susceptibility of the aromatic system to oxidative attack. As the reaction progresses, a marked decline in aromaticity is observed, indicating the formation of less complex intermediates, such as aliphatic compounds and low-molecular-weight carboxylic acids.

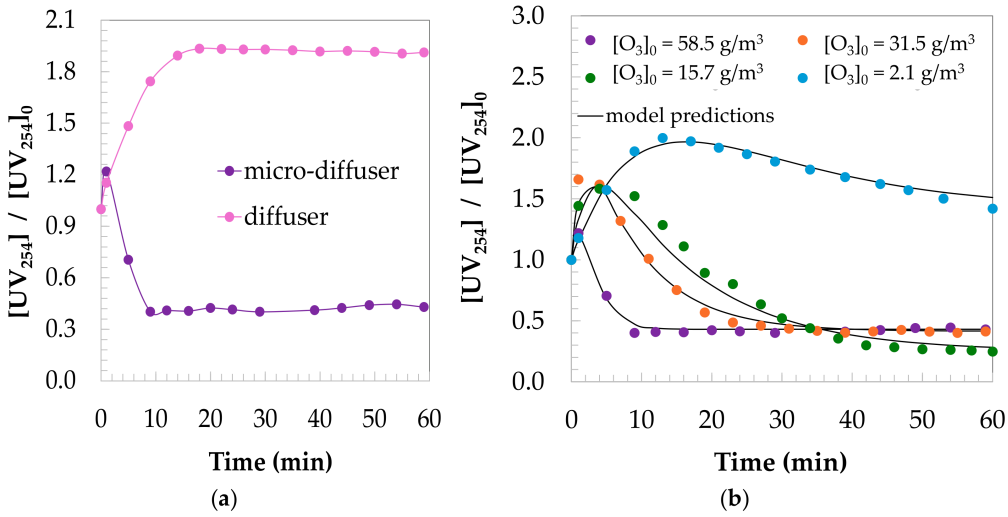

Figure 4. Loss of water aromaticity during CBZ ozonation: (**a**) effect of the ozone gas injection system operating at an ozone dosage of 58.8 g/m^3; (**b**) effect of the injected ozone dosage using a micro-diffuser. Experimental conditions: $[CBZ]_0$ = 50.0 mg/L; [T] = 25 °C; $[pH]_0$ = 10.3.

The use of a micro-diffuser generating microbubbles substantially enhances ozone mass transfer. These microbubbles provide a larger specific surface area and remain suspended in the liquid phase for longer periods, thereby increasing ozone solubilization and promoting its decomposition into hydroxyl radicals. These highly reactive species further accelerate the cleavage of conjugated double bonds within aromatic rings. As a result, aromaticity loss is faster and more pronounced, indicating a more efficient degradation of CBZ and enhanced formation of oxygenated intermediates.

This phenomenon is closely linked to the partial mineralization of the pollutant. However, the complete disappearance of aromaticity does not necessarily imply total removal of organic carbon, as oxygenated fragments may persist in solution. Nevertheless, the loss of aromatic character is considered a critical step toward water detoxification and the reduction in contaminant persistence.

Figure 4b presents the normalized aromaticity profiles as a function of the applied ozone mass flow rate during CBZ ozonation. When ozone concentrations between 15.7 and 58.5 g/m^3 are used, water aromaticity increases sharply within the first 3 min of reaction, reaching a maximum value. Both the time required to reach this maximum and its magnitude depend directly on the ozone dosage, indicating that the formation of oxygenated aromatic intermediates becomes more intense as ozone availability increases.

After reaching the maximum, aromaticity decreases with a steep slope and converges toward a stable value after approximately 40 min of treatment. This decline reflects the progressive oxidation and cleavage of the aromatic and conjugated structures formed during the initial stages of the process, which is favoured by the enhanced generation of hydroxyl radicals at high ozone concentrations.

In contrast, when ozonation is performed at a low ozone concentration (1.9 g/m^3), aromaticity exhibits a notably different behaviour. The maximum value is reached much later, around 15 min, and the subsequent decrease occurs slowly, following a near zero-

order kinetic trend. This indicates that under ozone-limited conditions, the formation and elimination of aromatic intermediates proceed more gradually, prolonging their persistence in the aqueous medium. Consequently, limited ozone availability slows aromatic ring cleavage and restricts the generation of radical species responsible for further oxidation and mineralization.

Overall, Figure 4b clearly reveals two distinct kinetic regimes: high ozone dosage regime (15.7–58.5 g/m^3), rapid formation and accelerated degradation of aromatic intermediates, characterized by steep kinetic profiles and short stabilization times; and low ozone dosage regime (1.9 g/m^3), slower accumulation and limited degradation of intermediates, exhibiting smoother, near zero-order kinetics and greater aromatic persistence.

The evolution of water aromaticity was described using a kinetic model based on a consecutive scheme of first-order reactions, in which CBZ is degraded into highly aromatic intermediate species. It was observed that the initial aromaticity of the aqueous solution containing CBZ increases during the early stages of the ozonation treatment, reaching a maximum aromaticity value. Once the maximum concentration of aromatic intermediates is generated in the aqueous phase, aromaticity subsequently decreases as a result of the degradation of these species, leading to the formation of final products of a non-aromatic nature. This reaction scheme can be represented as shown in Equation (5):

$$CBZ \overset{k_{Af}}{\rightarrow} Aromatic\ intermediates \overset{k_{Ad}}{\rightarrow} non-aromatic\ products \quad (5)$$

where k_{Af} and k_{Ad} are the apparent kinetic constants corresponding to the formation and destruction of aromatic intermediates (1/min), respectively. Both steps were assumed to follow first-order kinetics, a hypothesis commonly accepted in chemical and photochemical degradation systems when the oxidant is present in excess or can be considered constant over limited time intervals.

Unlike the classical approach for consecutive reactions, in this system the aromatic intermediates were assumed to exhibit a non-zero initial absorbance value, owing to the aromatic nature of the CBZ molecule, which contributes to the overall water aromaticity and was experimentally determined in the initial sample. Under these assumptions, the temporal evolution of the initial reactant (CBZ) is described by the differential equation corresponding to an irreversible first-order reaction, as shown in Equation (1), whose integration, applying the initial condition, leads to the exponential expression presented in Equation (3).

The differential equation describing the evolution of the aromatic intermediates is obtained by considering the balance between their formation rate from the initial reactant (CBZ) and their destruction rate toward final products. In its most general form, this equation can be written as shown in Equation (6):

$$\frac{d\,[UV_{254}]}{dt} = k_{Af}\,[CBZ] - r_d \quad (6)$$

where r_d (AU/min) represents the degradation rate of the aromatic intermediates. Experimentally, it was observed that water aromaticity does not tend toward zero at long reaction times, but instead reaches a constant residual value. This behaviour is attributed to the consumption or deactivation of the ozone responsible for their degradation, which results in the presence of a refractory aromatic fraction that cannot be further degraded under the experimental conditions. To account for this effect, it was assumed that only the degradable

fraction of the aromatic load follows first-order kinetics; therefore, the degradation rate of the aromatic intermediates can be expressed as

$$r_d = k_{Ad}\left([UV_{254}] - [UV_{254}]_{final}\right) \quad (7)$$

where ($[UV_{254}]_{final}$, AU) represents the residual aromatic concentration at long reaction times. By substituting this expression and the solution obtained for t into the differential equation of the intermediate, Equation (8) is obtained:

$$\frac{d[UV_{254}]}{dt} = k_{Af}\,[UV_{254,CBZ}]_0\,exp(-k_{Af}\,t) - k_{Ad}\left([UV_{254}] - [UV_{254}]_{final}\right) \quad (8)$$

The resulting analytical solution for the concentration of aromatic intermediates as a function of time is given by Equation (9):

$$[UV_{254}] = \frac{k_{Af}\,[UV_{254,CBZ}]_0}{k_{Ad} - k_{Af}}\,[exp(-k_{Af}\,t) - exp(-k_{Ad}\,t)] + ([UV_{254}]_0 - [UV_{254}]_{final})\,exp(-k_{Ad}\,t) + [UV_{254}]_{final} \quad (9)$$

$$k_{Af} = -0.0003\,[O_3]_0^2 + 0.0272\,[O_3]_0 + 0.0212 \quad (10)$$

$$k_{Ad} = 0.0002\,[O_3]_0^2 - 0.0058\,[O_3]_0 + 0.0959 \quad (11)$$

The estimated kinetic parameters are reported in Table 1, while the model predictions are shown in Figure 4b. The obtained expression fully and consistently describes the evolution of aromatic intermediates in the system. The first term accounts for the transient formation of aromatic intermediates from CBZ and their subsequent degradation; the second term represents the decay of the initially present aromatic fraction that is susceptible to degradation; whereas the third term corresponds to the refractory aromatic fraction that remains in the system once the oxidant has been depleted.

3.3.2. Formation and Decay of Colored Intermediates

Figure 5a illustrates the evolution of water color during CBZ ozonation. The initial aqueous CBZ solution is colorless. When a conventional diffuser is employed, ozone mass transfer to the liquid phase is relatively inefficient due to the limited interfacial area of the larger bubbles and their rapid ascent within the reactor. As a consequence, reaction rates are slower because the concentration of dissolved ozone remains low, and no visible color development is observed in the solution. This indicates that CBZ does not undergo degradation pathways leading to the formation of colored intermediates under these conditions.

In contrast, the use of a micro-diffuser generates microbubbles that enhance ozone solubilization and extend gas–liquid contact time, thereby promoting CBZ degradation through oxidative pathways that lead to the formation of colored intermediate compounds. As observed in Figure 5a, the maximum color intensity appears approximately 5 min after the start of ozonation, resulting in a bright yellow aqueous solution.

This yellow coloration arises from the formation of oxygenated aromatic intermediates containing conjugated systems capable of absorbing visible light. Among the main intermediates identified during CBZ degradation by ozone and hydroxyl radicals are oxygenated aromatic heterocyclic compounds (benzotriazole-type derivatives), polycyclic aromatic nitrogen-containing oxidation products (acridine/acridone-type compounds), primary oxygenated carbamazepine derivatives (hydroxy- and epoxy-CBZ), and other conjugated aromatic oxidation intermediates. These species typically contain partially opened or oxygenated aromatic rings, bearing functional groups such as aldehydes, enones, or conjugated heterocyclic moieties, which are responsible for the observed yellow coloration.

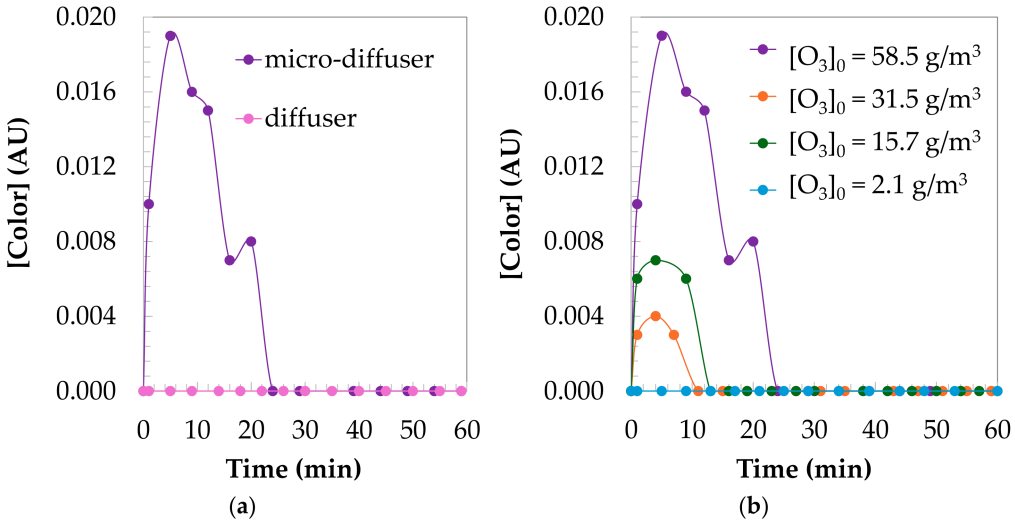

Figure 5. Color changes in ozonated aqueous CBZ solutions: (**a**) effect of the ozone gas injection system operating at an ozone dosage of 58.8 g/m^3; (**b**) effect of the injected ozone dosage using a micro-diffuser. Experimental conditions: $[CBZ]_0$ = 50.0 mg/L; [T] = 25 °C; $[pH]_0$ = 10.3.

Once the formation of colored intermediates reaches its maximum, the increased generation of hydroxyl radicals in the presence of microbubbles leads to their progressive degradation. This process involves the cleavage of conjugated systems responsible for visible light absorption, resulting in a gradual reduction in color intensity. This discoloration is associated with the breakdown of aromatic ring structures and the formation of more highly oxygenated, less chromophoric products, such as short-chain carboxylic acids and other low-molecular-weight compounds. Therefore, the disappearance of color can be considered an indirect indicator of the removal of aromatic and chromophoric structures formed during CBZ degradation. Figure 5b shows the evolution of water color during CBZ ozonation as a function of the applied ozone dosage using a micro-diffuser. As observed, the initial solution is colorless; however, upon initiating ozonation, a characteristic yellow color rapidly develops. This coloration appears within the first 5 min of reaction, and its intensity increases with the applied ozone mass flow rate, indicating that higher ozone availability favors the formation of chromophoric intermediates derived from partial CBZ oxidation.

The higher color intensity observed at elevated ozone dosages suggests that oxygenated aromatic intermediates with conjugated systems are formed more rapidly and in greater amounts under these conditions. After reaching a maximum, the color intensity decreases sharply until it disappears, indicating the subsequent degradation of these intermediates. This decay is promoted by the increased presence of hydroxyl radicals when dissolved ozone concentrations are high.

Notably, when CBZ ozonation is carried out at low ozone gas concentrations, on the order of 2.1 g/m^3, no visible color formation is detected in the aqueous phase. This behaviour suggests that under ozone-limited conditions, CBZ degradation proceeds slowly and chromophoric intermediates do not accumulate to detectable levels. In contrast, ozone dosages above 15.7 g/m^3 are required for observable color development, revealing a clear dependence of the process on ozone availability.

At the highest ozone dosage tested (58.5 g/m^3), the maximum color intensity is achieved, and the yellow coloration persists for approximately 25 min before disappearing. This extended persistence is associated with the rapid generation of aromatic intermediates during the early stages of the process, followed by their gradual oxidation and degradation through the progressive cleavage of conjugated systems responsible for coloration.

Overall, the results presented in Figure 5 demonstrate that the formation and disappearance of color constitute a highly sensitive and informative indirect indicator of CBZ oxidation progress. High ozone flow rates promote greater formation and longer temporal persistence of color due to rapid generation of chromophoric intermediates, whereas low ozone flow rates result in the absence of visible color, reflecting slower oxidative pathways and limited accumulation of aromatic intermediates.

3.3.3. Turbidity Development in Ozonated CBZ Solutions

As shown in Figure 6a, water turbidity does not exhibit significant variations during CBZ ozonation, regardless of the ozone injection system used. It is worth noting that, in all cases, turbidity values remain below 5 NTU, which is the maximum limit established by the World Health Organization (WHO) for water to be considered suitable for use, including irrigation and other non-potable applications. According to WHO guidelines, water intended for human consumption should not exceed this 5 NTU threshold, and ideally should remain below 1 NTU under standard drinking water treatment conditions. Therefore, the values observed when using a micro-diffuser fall well within acceptable limits, even under more restrictive quality standards.

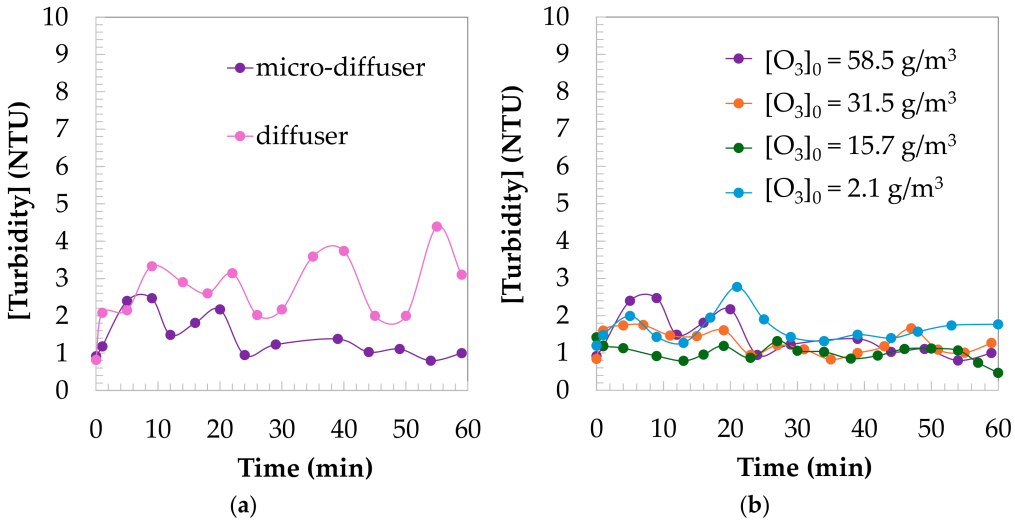

Figure 6. Evolution of water turbidity during CBZ ozonation: (**a**) effect of the ozone gas injection system operating at an ozone dosage of 58.8 g/m^3; (**b**) effect of the injected ozone dosage using a micro-diffuser. Experimental conditions: $[CBZ]_0$ = 50.0 mg/L; [T] = 25 °C; $[pH]_0$ = 10.3.

The stability of turbidity throughout the process indicates that CBZ ozonation, despite generating degradation intermediates, does not lead to the formation of suspended particles or colloidal matter in amounts sufficient to impair water clarity. This suggests that the intermediates produced are predominantly soluble and do not contribute significantly to light scattering, which is reflected in the nearly constant NTU values. Consequently, turbidity measurements confirm that ozonation does not promote coagulation, precipitation, or aggregation phenomena that could adversely affect the physical quality of the treated water.

Figure 6b depicts the evolution of water turbidity as a function of ozone dosage during CBZ ozonation. The results show that, for all ozone concentrations tested, turbidity values remain below 3 NTU. These values are well below the maximum limit of 5 NTU established by the WHO for agricultural water use, further confirming that ozonation under the applied conditions does not generate suspended particles or colloidal structures that deteriorate water quality.

This behaviour indicates that the intermediates formed during CBZ oxidation are largely soluble and do not tend to aggregate or precipitate, even at higher ozone flow rates. In addition, the stable turbidity values suggest that ozonation does not induce coagulation processes, micelle formation, or the release of fine solids that could increase light scattering. Therefore, the data presented in Figure 6 confirm that, from a turbidity perspective, the treated water retains suitable physical characteristics for agricultural reuse, independently of the ozone concentration applied.

3.4. Dissolved Ozone Dynamics and Oxidant Availability

A detailed understanding of ozone behaviour during the ozonation process is essential to elucidate the mechanisms governing contaminant degradation and to evaluate process efficiency. In this section, the dynamics of ozone transfer from the gas phase to the aqueous phase are analyzed, considering both physical and chemical aspects of the process. First, the evolution of ozone concentration in the gas phase is examined to assess ozone utilization and losses. Subsequently, the dissolved ozone concentration in water is discussed as a key parameter controlling oxidation reactions.

3.4.1. Ozone Concentration in the Gas Phase

Figure 7a illustrates the temporal evolution of ozone concentration in the gas phase during CBZ ozonation. As can be observed, the ozone concentration in the gas phase initially decreases during the first 2 min of ozonation and subsequently increases until it reaches a steady value corresponding to the inlet ozone concentration in the contactor, which is attained after approximately 15 min. The lowest gas-phase ozone concentration is observed when a micro-diffuser is employed, whereas a less pronounced decrease is detected when a conventional gas injector is used.

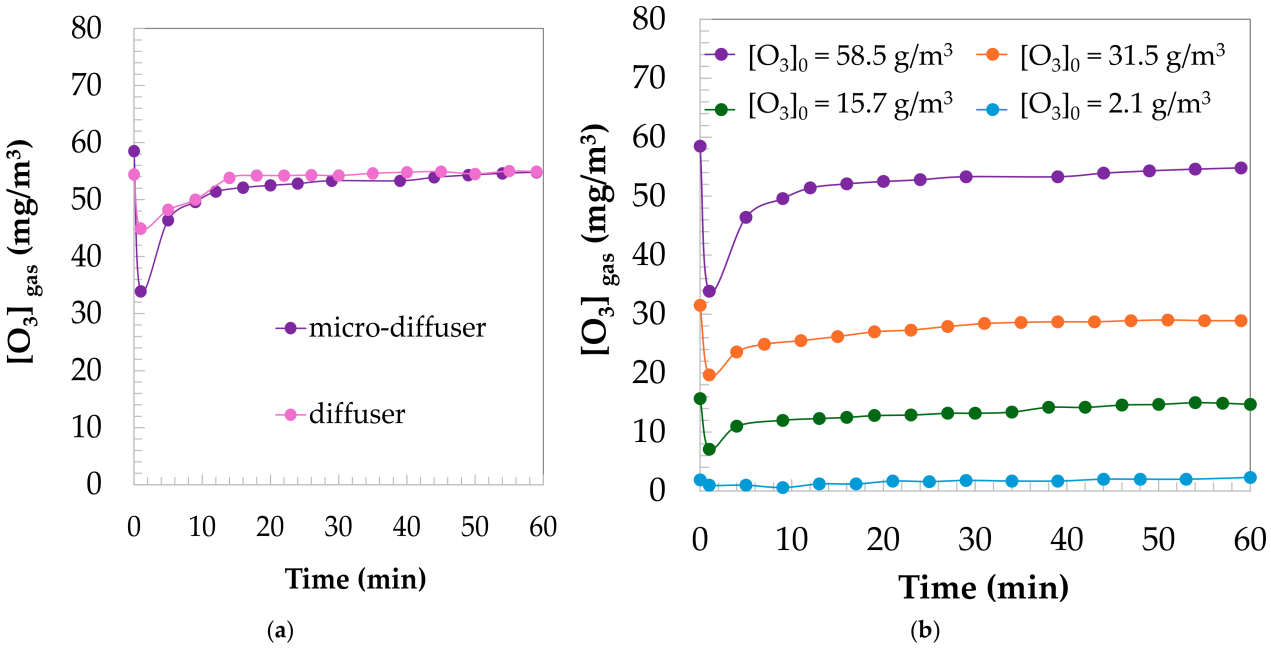

Figure 7. Concentration of ozone in the gas phase during CBZ ozonation: (**a**) effect of the ozone gas injection system operating at an ozone dosage of 58.8 g/m^3; (**b**) effect of the injected ozone dosage using a micro-diffuser. Experimental conditions: $[CBZ]_0$ = 50.0 mg/L; [T] = 25 °C; $[pH]_0$ = 10.3.

This behaviour can be explained by the differences in gas–liquid mass transfer efficiency between the two injection systems. The micro-diffuser generates microbubbles with a very high interfacial area and a longer residence time within the reactor. As a result,

ozone is transferred to the aqueous phase more efficiently, where it rapidly dissolves and is immediately consumed in the oxidation reactions of CBZ and its intermediate products. This enhanced transfer and reaction rate causes a sharper initial decrease in the ozone concentration in the gas phase, as the available ozone is quickly incorporated into the liquid phase and reacts almost instantaneously.

In contrast, when a conventional injector is used, the generated bubbles are larger, rise more rapidly through the reactor, and exhibit a lower specific surface area. These characteristics limit the amount of ozone transferred to the liquid phase during the initial stage of ozonation. Consequently, the initial decrease in gas-phase ozone concentration is less pronounced, and a larger fraction of the unabsorbed ozone exits the reactor through the off-gas.

After the initial period, a similar trend is observed for both injection systems. As CBZ and its oxidizable intermediates become progressively depleted, the chemical demand for ozone decreases. Accordingly, the gas-phase ozone concentration gradually recovers and approaches the inlet ozone concentration, indicating that the system has reached a dynamic balance between gas–liquid mass transfer and chemical consumption.

Figure 7b presents the evolution of the gas-phase ozone concentration inside the reactor as a function of the applied inlet ozone concentration during CBZ ozonation. In all cases, a marked decrease in gas-phase ozone concentration is observed within the first 2 min of reaction, reaching a characteristic minimum during this initial stage. This sharp decline is attributed to the high oxidant demand of the system, in which both CBZ and the early oxidation intermediates react rapidly with the ozone transferred from the gas phase into the aqueous phase.

Subsequently, the gas-phase ozone concentration increases progressively as CBZ degradation advances and the oxidizing capacity of the medium diminishes. This increase continues until, after approximately 20 min of operation, the ozone concentration in the gas phase becomes very close to the inlet ozone concentration supplied to the system. This behaviour indicates that an equilibrium has been established between gas–liquid ozone transfer and oxidant consumption.

Overall, these results confirm that the system operates under two clearly differentiated regimes: an initial high oxidant-demand regime, in which the transferred ozone is rapidly consumed and the gas-phase ozone concentration decreases sharply; and a subsequent saturation or quasi-equilibrium regime, in which the oxidant demand of the medium is substantially reduced, allowing ozone to accumulate in both the gas phase and the aqueous solution, ultimately stabilizing at values close to the inlet ozone concentration.

3.4.2. Dissolved Ozone Concentration in Water

Figure 8a shows the temporal evolution of dissolved ozone concentration in water, a critical parameter governing the effectiveness of the ozonation process. When a conventional diffuser is employed, the dissolved ozone concentration increases slowly after approximately 25 min of reaction and reaches maximum values of around 2.0 mg/L, which limits the oxidation rate of CBZ. In contrast, the use of a micro-diffuser enables much more efficient ozone transfer, achieving dissolved ozone concentrations above 20.0 mg/L within 10 min. This not only enhances ozone availability for direct oxidation reactions but also promotes the formation of hydroxyl radicals, thereby accelerating CBZ degradation and the mineralization of its oxidation intermediates.

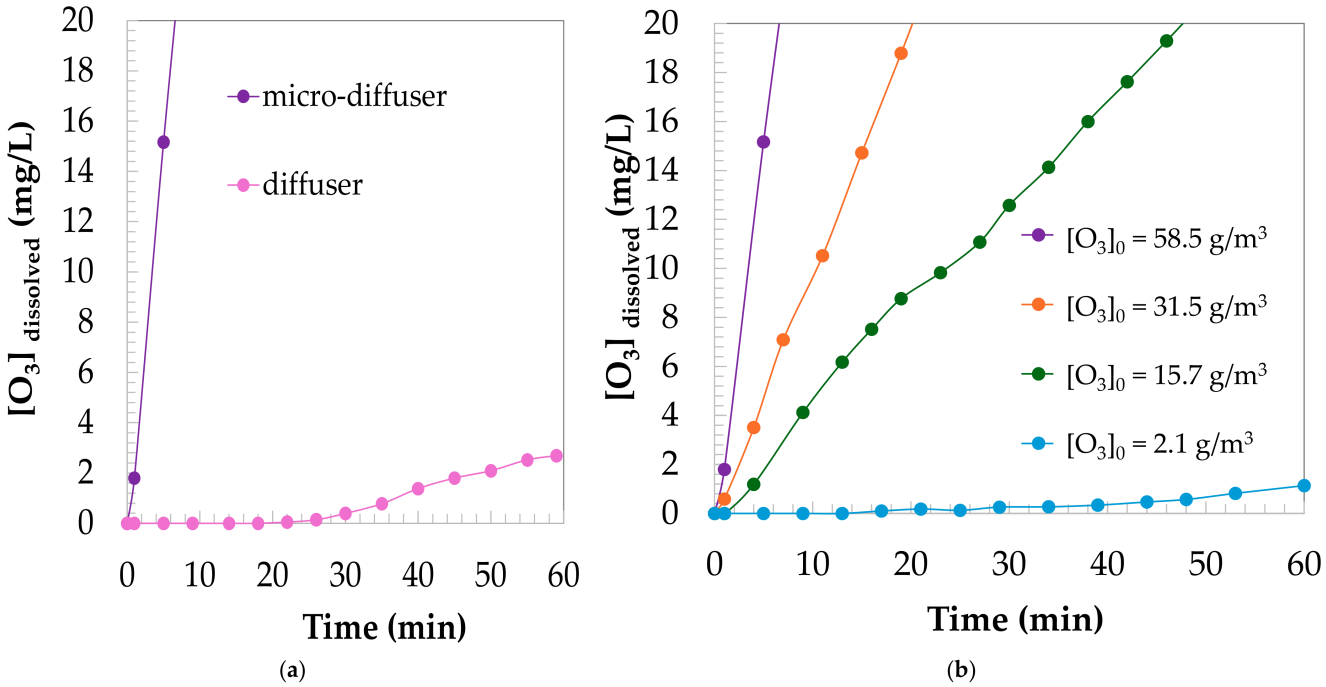

Figure 8. Concentration of dissolved ozone in water during CBZ ozonation: (**a**) effect of the ozone gas injection system operating at an ozone dosage of 58.8 g/m^3; (**b**) effect of the injected ozone dosage using a micro-diffuser. Experimental conditions: $[CBZ]_0$ = 50.0 mg/L; [T] = 25 °C; $[pH]_0$ = 10.3.

This behaviour highlights the marked differences in gas–liquid mass transfer efficiency between the two injection systems. The generation of microbubbles significantly increases the gas–liquid interfacial area and prolongs ozone residence time within the reactor, favouring rapid and continuous dissolution. As a result, high dissolved ozone concentrations are attained at very short reaction times, creating a strongly oxidative environment in which both selective oxidation pathways driven by molecular ozone and non-selective reactions mediated by hydroxyl radicals play a dominant role.

It is worth emphasizing that the high dissolved ozone concentrations observed when using the micro-diffuser markedly accelerate aromatic ring cleavage and the degradation of chromophoric intermediates formed during the early stages of ozonation. This, in turn, promotes progressive mineralization toward more oxygenated, lower-molecular-weight compounds, effectively reducing the overall organic load of the water. Therefore, the evolution of dissolved ozone concentration confirms that the use of a micro-diffuser not only intensifies the process but also allows the reactor to operate under more efficient conditions with improved control over oxidation pathways.

Figure 8b presents the evolution of dissolved ozone concentration during CBZ ozonation as a function of the applied inlet ozone concentration. As shown, the dissolved ozone concentration increases almost linearly with time, with the slope of this increase being directly dependent on the ozone concentration supplied in the gas phase. Higher inlet ozone concentrations lead to higher gas–liquid transfer rates and, consequently, higher dissolved ozone levels during treatment.

This behaviour indicates that, under the studied conditions, the process operates in a regime in which gas–liquid mass transfer is the limiting step. As the gas-phase ozone concentration increases, the driving force for transfer between the two phases becomes larger, thereby enhancing oxidant absorption. This effect is reflected in the steeper slopes observed at higher ozone dosages, suggesting that ozone is not immediately consumed by CBZ or its intermediates and that part of the oxidant progressively accumulates in the aqueous phase.

For all ozone dosages investigated, the temporal evolution of dissolved ozone deviates from the behaviour expected for a purely mass-transfer-controlled process, indicating that ozone dissolution is continuously coupled with chemical consumption. Under the experimental conditions investigated, no temporal domain could be identified in which ozone accumulation followed a purely physical absorption behaviour. Therefore, the estimation of an intrinsic volumetric mass-transfer coefficient was not pursued, as such a parameter would lack physical meaning in a system dominated by simultaneous mass transfer and fast chemical reaction.

4. Discussion

The present study provides a comprehensive mechanistic interpretation of carbamazepine ozonation. It explicitly links reaction kinetics, oxidant availability, and transformation pathways across a wide range of ozone dosages. While similar degradation trends have been previously reported for CBZ and related compounds, these studies often do not explicitly address the role of regime transitions or the coupling between mass transfer and reaction kinetics, which are shown here to be key factors governing system behaviour. In this regard, it is important to emphasize that the kinetic model presented here is based on parameter estimation from experimental data and validated through regression analysis, rather than on qualitative trend interpretation alone.

The scientific value of this study lies not in the mere observation of contaminant degradation, but in the systematic identification of kinetic regimes and their mechanistic interpretation as a function of ozone supply. This approach provides insights that are directly relevant for process optimization and scale-up, distinguishing this work from conventional degradation studies that typically operate under fixed or excess oxidant conditions without addressing regime transitions. Importantly, this study goes beyond a purely descriptive analysis of degradation behaviour, as it links experimental observations to a coherent mechanistic interpretation based on oxidant availability and coupled mass transfer–reaction phenomena. This approach allows the identification of governing parameters and provides a generalizable framework for understanding and optimizing contaminant–oxidant systems.

In contrast to conventional studies on ozonation and other advanced oxidation processes, which generally assume a single kinetic regime, the present work demonstrates that contaminant degradation may occur under distinct and operatively relevant regimes controlled by oxidant supply conditions, highlighting the importance of explicitly considering regime transitions for process interpretation and optimization.

The results demonstrate that CBZ degradation does not occur under a single, well-defined kinetic regime, but rather under coupled mass-transfer–reaction regimes in which physical ozone dissolution and chemical consumption take place simultaneously. This behaviour is particularly evident from the dissolved ozone profiles, which show that ozone accumulation in the aqueous phase is continuously counterbalanced by rapid reaction with CBZ and its oxidation intermediates. Consequently, the use of classical intrinsic mass-transfer coefficients is insufficient to describe system performance, and a regime-based interpretation is more appropriate for understanding and optimizing ozonation-based advanced oxidation processes.

The observed linear dependence of the apparent pseudo-first-order rate constant on the inlet ozone concentration reflects oxidant availability under the studied conditions in a coupled mass transfer–reaction system, and does not represent an intrinsic kinetic rate law. At low ozone dosages, the system operates under an ozone-limited regime, characterized by slow CBZ degradation, delayed pH evolution, and prolonged persistence of aromatic intermediates. Under these conditions, molecular ozone is rapidly consumed upon dissolu-

tion, and the generation of secondary reactive species, such as hydroxyl radicals, remains limited. As the inlet ozone concentration increases beyond a threshold (≈15.7 g/m^3 under the studied conditions), the system transitions to a high-oxidant regime, where CBZ degradation becomes reaction-controlled rather than oxidant-limited. In this regime, high dissolved ozone levels and enhanced radical formation result in rapid CBZ disappearance, accelerated aromatic ring cleavage, and fast transformation of intermediate compounds.

The evolution of pH provides additional insight into the degradation mechanisms and corroborates the existence of distinct kinetic regimes. The rapid decrease in pH observed at high ozone dosages reflects the intense formation of low-molecular-weight carboxylic acids derived from aromatic ring opening and subsequent oxidation steps. The stabilization of pH around 4.3 indicates that, once the main organic load has been oxidized, the aqueous system becomes governed by the $CO_2/H_2CO_3/HCO_3^-$ equilibrium resulting from partial mineralization. In contrast, the gradual pH decrease observed under ozone-limited conditions indicates slower acid formation and highlights the reduced oxidative capacity of the system when oxidant supply is insufficient.

Monitoring changes in aromaticity and color revealed the transient nature of oxidation intermediates and provided valuable information on CBZ transformation pathways. The initial increase in UV_{254} absorbance and the formation of yellow-colored solutions under high ozone dosages indicate the accumulation of oxygenated aromatic intermediates containing conjugated structures. The subsequent decay of both aromaticity and color signals demonstrates that these intermediates are not stable end-products but are progressively degraded as ozone and hydroxyl radicals continue to act. This observation is relevant from a water quality perspective, as it confirms that the formation of potentially hazardous aromatic by-products is temporary and strongly dependent on maintaining sufficient oxidant availability to drive their further oxidation.

The behaviour of transient oxidation intermediates observed in this study is consistent with previous reports on carbamazepine ozonation, where the formation of oxygenated aromatic compounds and epoxide derivatives has been widely documented. However, previous studies have mainly focused on identifying transformation products rather than linking their formation and decay to operating conditions. In contrast, the present results demonstrate that the generation and subsequent degradation of these intermediates are strongly governed by ozone availability and kinetic regime.

However, unlike most previous studies, which primarily focus on the identification of transformation products or overall removal efficiencies under fixed operating conditions, the present work provides a process-oriented interpretation that explicitly links these observations to oxidant availability and kinetic regime transitions. This distinction is important, as it moves beyond descriptive analysis and enables a more general understanding of how operating parameters govern both reaction rates and transformation pathways in ozonation systems.

From a practical perspective, this finding has important implications for water treatment applications. The transient accumulation of aromatic and chromophoric intermediates indicates the presence of incomplete oxidation stages may temporarily increase the presence of potentially reactive or undesirable species. Therefore, maintaining sufficient oxidant availability and appropriate contact time is essential to ensure their further degradation and to avoid discharge of partially oxidized by-products. This highlights the importance of controlling ozone dosage not only for pollutant removal efficiency but also for ensuring the effective transformation and minimization of intermediate species in full-scale treatment systems.

In addition, several practical limitations should be considered. The performance of the process is strongly dependent on gas–liquid mass transfer efficiency, which may be

reduced at large scale due to hydrodynamic constraints. Furthermore, the presence of natural organic matter, inorganic species, and radical scavengers in real water matrices can significantly increase ozone demand and alter reaction pathways. The transient accumulation of oxidation intermediates also requires careful control of ozone dosage and contact time to ensure their complete degradation. Finally, although the mechanistic trends identified are transferable, the use of elevated CBZ concentrations for analytical purposes may lead to differences in absolute kinetics under environmentally relevant conditions.

The mechanistic interpretation presented in this study is primarily based on indirect analytical indicators, including UV_{254} absorbance, color evolution, and pH changes, rather than on direct identification of transformation products by advanced techniques such as LC–MS. However, this approach is supported by extensive literature describing the ozonation pathways of carbamazepine and structurally related compounds.

Previous studies have demonstrated that CBZ ozonation proceeds through well-established reaction mechanisms involving the rapid formation of epoxide intermediates, followed by successive oxidation steps leading to hydroxylated derivatives, quinones, and ultimately low-molecular-weight carboxylic acids. These pathways are associated with characteristic changes in aromaticity, chromophoric properties, and solution acidity, which are consistent with the experimental observations reported in this work.

Therefore, the evolution of UV_{254} absorbance, color formation and decay, and pH profiles can be reliably interpreted as indirect signatures of intermediate formation and degradation, providing meaningful mechanistic insight into the oxidation process. In this case, the combination of kinetic analysis with physicochemical indicators represents a robust and widely accepted approach for elucidating reaction pathways in advanced oxidation processes when direct identification of all intermediates is not feasible.

Notably, turbidity remained low and stable throughout all experiments, suggesting that CBZ ozonation does not promote the formation of insoluble by-products or colloidal aggregates. This finding implies that the oxidation pathways predominantly yield soluble intermediates and end-products, preserving the physical quality of the treated water and supporting the suitability of ozonation as a polishing or tertiary treatment step.

From a broader perspective, the kinetic and mechanistic framework developed in this work establishes chemical ozonation as a robust reference process for evaluating more complex advanced oxidation systems. Future research should focus on coupling this regime-based kinetic approach with nanomaterials-enabled photocatalysis under irradiation, enabling the systematic evaluation of synergies, energy efficiency, and transformation pathways in next-generation hybrid AOPs. In particular, the quantitative relationships between ozone dosage, reaction rates, and intermediate dynamics provide a valuable benchmark for assessing the true added value of nanomaterials-assisted photocatalytic and hybrid ozone–photocatalytic systems. This perspective contributes to bridging the gap between empirical observations and mechanistic understanding in advanced oxidation processes, reinforcing the relevance of the present results beyond the specific system studied.

From a practical standpoint, scaling up ozonation processes from a laboratory to industrial scale involves several challenges. In real systems, gas–liquid mass transfer efficiency may be reduced due to hydrodynamic limitations, affecting ozone dissolution and overall process performance. In addition, the presence of natural organic matter, inorganic ions, and radical scavengers can increase ozone demand and alter reaction pathways, potentially reducing treatment efficiency. Operational aspects such as ozone generation costs, energy consumption, and reactor design must also be considered to ensure process viability. Furthermore, the transient accumulation of oxidation intermediates highlights the need for sufficient contact time and appropriate oxidant dosage to achieve complete transformation. In this case, the identification of kinetic regimes and the quantitative

relationship between ozone concentration and reaction rate obtained in this study provide a valuable basis for scaling up and optimizing ozone-based and hybrid advanced oxidation processes under realistic operating conditions.

At the same time, the present study does not propose a novel treatment technology, but rather provides a mechanistic and kinetic framework for optimizing a well-established process. In this sense, the identification of kinetic regimes and their dependence on ozone concentration offers practical criteria for process design and operation, including the selection of appropriate ozone dosages, optimization of gas–liquid contact efficiency, and definition of adequate contact times. These aspects are directly relevant for full-scale ozonation systems, where oxidant transfer and consumption are key limiting factors.

5. Conclusions

Carbamazepine ozonation operates under coupled transfer–reaction regimes across the entire range of ozone dosages investigated, with ozone concentration emerging as the key parameter governing reaction kinetics and transformation pathways. The linear dependence of the apparent first-order rate constant on inlet ozone concentration, together with dissolved ozone and pH dynamics, demonstrates a clear transition from ozone-limited to reaction-controlled regimes at concentrations ≥ 15.7 g/m^3. The transient formation and subsequent degradation of aromatic and chromophoric intermediates confirm that oxidation by-products are not persistent when sufficient oxidant availability is maintained. Beyond the specific case of CBZ ozonation, the regime-based interpretation proposed in this work constitutes a generalizable conceptual framework applicable to other contaminant–oxidant systems, in which oxidant availability and mass transfer jointly determine reaction kinetics and transformation pathways.

From an applied perspective, these findings provide a mechanistic framework for optimizing ozone dosage, reactor operation, and contact time in water treatment processes. Furthermore, the results offer a valuable benchmark for the design and evaluation of hybrid advanced oxidation systems. Future work should focus on validation under environmentally relevant conditions and the assessment of transformation product toxicity to support safe and efficient large-scale implementation. Here, the proposed framework is directly applicable to real water treatment systems, supporting scale-up by linking ozone dosage, mass transfer, and reaction kinetics under practical operating conditions.

From a fundamental perspective, the results show that carbamazepine ozonation cannot be described by a single kinetic regime. Instead, it involves a dynamic interplay between mass transfer and a chemical reaction. The identification of a transition between ozone-limited and reaction-controlled regimes provides a validated mechanistic basis for interpreting apparent kinetic behavior in reactive gas–liquid systems. In this context, the apparent pseudo-first-order constants determined in this work should be understood as integrated parameters reflecting both oxidant availability and system hydrodynamics. Moreover, the combined analysis of CBZ degradation, dissolved ozone dynamics, pH evolution, and spectroscopic indicators demonstrates that oxidation pathways and intermediate formation are strongly dependent on operating conditions. This highlights the importance of considering not only pollutant removal but also the evolution and fate of transformation products when evaluating advanced oxidation processes.

Author Contributions: Conceptualization, N.V.; methodology, M.A.V.-C., U.D. and E.B.-G.; software, M.A.V.-C., E.B.-G., U.D. and N.V.; validation, M.A.V.-C., E.B.-G., U.D. and N.V.; formal analysis, M.A.V.-C., E.B.-G., U.D. and N.V.; investigation, M.A.V.-C., E.B.-G. and N.V.; resources, M.A.V.-C., E.B.-G. and N.V.; data curation, M.A.V.-C., E.B.-G., U.D. and N.V.; writing—original draft preparation, E.B.-G. and N.V.; writing—review and editing, N.V.; visualization, E.B.-G., U.D. and N.V.; supervision,

N.V.; project administration, N.V.; funding acquisition, N.V. All authors have read and agreed to the published version of the manuscript.

Funding: This research was funded by PIBA_2023_01_0032—Basic and/or Applied Research Project. Financing entity: Basque Government 2023.

Institutional Review Board Statement: Not applicable.

Informed Consent Statement: Not applicable.

Data Availability Statement: The database is available upon request.

Acknowledgments: The authors thank the Department of Chemical and Environmental Engineering and the Department of Chemical Engineering of the University of the Basque Country UPV/EHU for their support.

Conflicts of Interest: The authors declare no conflicts of interest.

References

1. Heberer, T. Occurrence, fate, and removal of pharmaceutical residues in the aquatic environment: A review of recent research data. *Toxicol. Lett.* **2002**, *131*, 5–17. [CrossRef]
2. Wilkinson, J.L.; Boxall, A.B.A.; Kolpin, D.W.; Leung, K.M.Y.; Lai, R.W.S.; Galbán-Malagón, C.; Adell, A.D.; Mondon, J.; Metian, M.; Marchant, R.A.; et al. Pharmaceutical pollution of the world's rivers. *Proc. Natl. Acad. Sci. USA* **2022**, *119*, e2113947119. [CrossRef]
3. Clara, M.; Strenn, B.; Kreuzinger, N. Carbamazepine as a possible anthropogenic marker in the aquatic environment: Investigations on the behaviour of Carbamazepine in wastewater treatment and during groundwater infiltration. *Water Res.* **2004**, *38*, 947–954. [CrossRef] [PubMed]
4. Miao, X.-S.; Yang, J.-J.; Metcalfe, C.D. Carbamazepine and Its Metabolites in Wastewater and in Biosolids in a Municipal Wastewater Treatment Plant. *Environ. Sci. Technol.* **2005**, *39*, 7469–7475. [CrossRef]
5. Zhang, Y.; Geissen, S.-U.; Gal, C. Carbamazepine and diclofenac: Removal in wastewater treatment plants and occurrence in water bodies. *Chemosphere* **2008**, *73*, 1151–1161. [CrossRef]
6. Onesios, K.M.; Yu, J.T.; Bouwer, E.J. Biodegradation and removal of pharmaceuticals and personal care products in treatment systems: A review. *Biodegradation* **2009**, *20*, 441–466. [CrossRef] [PubMed]
7. Joss, A.; Keller, E.; Alder, A.C.; Göbel, A.; McArdell, C.S.; Ternes, T.; Siegrist, H. Removal of pharmaceuticals and fragrances in biological wastewater treatment. *Water Res.* **2005**, *39*, 3139–3152. [CrossRef]
8. Verlicchi, P.; Al Aukidy, M.; Zambello, E. Occurrence of pharmaceutical compounds in urban wastewater: Removal, mass load and environmental risk after a secondary treatment—A review. *Sci. Total Environ.* **2012**, *429*, 123–155. [CrossRef]
9. Vieno, N.; Tuhkanen, T.; Kronberg, L. Elimination of pharmaceuticals in sewage treatment plants in Finland. *Water Res.* **2007**, *41*, 1001–1012. [CrossRef] [PubMed]
10. Escher, B.I.; Pronk, W.; Suter, M.J.F.; Maurer, M. Monitoring the Removal Efficiency of Pharmaceuticals and Hormones in Different Treatment Processes of Source-Separated Urine with Bioassays. *Environ. Sci. Technol.* **2006**, *40*, 5095–5101. [CrossRef]
11. Funke, J.; Prasse, C.; Ternes, T.A. Identification of transformation products of antiviral drugs formed during biological wastewater treatment and their occurrence in the urban water cycle. *Water Res.* **2016**, *98*, 75–83. [CrossRef]
12. Hollender, J.; Zimmermann, S.G.; Koepke, S.; Krauss, M.; McArdell, C.S.; Ort, C.; Singer, H.; von Gunten, U.; Siegrist, H. Elimination of Organic Micropollutants in a Municipal Wastewater Treatment Plant Upgraded with a Full-Scale Post-Ozonation Followed by Sand Filtration. *Environ. Sci. Technol.* **2009**, *43*, 7862–7869. [CrossRef]
13. Miklos, D.B.; Remy, C.; Jekel, M.; Linden, K.G.; Drewes, J.E.; Hübner, U. Evaluation of advanced oxidation processes for water and wastewater treatment—A critical review. *Water Res.* **2018**, *139*, 118–131. [CrossRef]
14. Issaka, E.; Amu-Darko, J.N.-O.; Yakubu, S.; Fapohunda, F.O.; Ali, N.; Bilal, M. Advanced catalytic ozonation for degradation of pharmaceutical pollutants—A review. *Chemosphere* **2022**, *289*, 133208. [CrossRef] [PubMed]
15. Dai, M.; Niu, Q.; Wu, S.; Lin, Y.; Biswas, J.K.; Yang, C. Hydroxyl radicals in ozone-based advanced oxidation of organic contaminants: A review. *Environ. Chem. Lett.* **2024**, *22*, 3059–3106. [CrossRef]
16. Huber, M.M.; Canonica, S.; Park, G.-Y.; von Gunten, U. Oxidation of Pharmaceuticals during Ozonation and Advanced Oxidation Processes. *Environ. Sci. Technol.* **2003**, *37*, 1016–1024. [CrossRef]
17. Lim, S.; Shi, J.L.; von Gunten, U.; McCurry, D.L. Ozonation of organic compounds in water and wastewater: A critical review. *Water Res.* **2022**, *213*, 118053. [CrossRef]
18. Lee, Y.; von Gunten, U. Oxidative transformation of micropollutants during municipal wastewater treatment: Comparison of kinetic aspects of selective (chlorine, chlorine dioxide, ferrateVI, and ozone) and non-selective oxidants (hydroxyl radical). *Water Res.* **2010**, *44*, 555–566. [CrossRef] [PubMed]

19. Nawrocki, J.; Kasprzyk-Hordern, B. The efficiency and mechanisms of catalytic ozonation. *Appl. Catal. B* **2010**, *99*, 27–42. [CrossRef]
20. Beltrán, F.J. *Ozone Reaction Kinetics for Water and Wastewater Systems*; CRC Press: Boca Raton, FL, USA, 2003. [CrossRef]
21. McDowell, D.C.; Huber, M.M.; Wagner, M.; von Gunten, U.; Ternes, T.A. Ozonation of Carbamazepine in Drinking Water: Identification and Kinetic Study of Major Oxidation Products. *Environ. Sci. Technol.* **2005**, *39*, 8014–8022. [CrossRef]
22. Attia, M.S.; Abdel-Wahed, M.S.; Algethami, F.K.; El-Kalliny, A.S. Advanced oxidation processes (AOPs) for drinking water treatment: A state-of-the-art review on applications, efficacy, and implementation challenges. *RSC Adv.* **2026**, *16*, 22186–22203. [CrossRef]
23. Mahmoodi, M.; Pishbin, E. Ozone-based advanced oxidation processes in water treatment: Recent advances, challenges, and perspective. *Environ. Sci. Pollut. Res.* **2025**, *32*, 3531–3570. [CrossRef]
24. Cardoso, R.M.F.; Esteves da Silva, J.C.G.; Pinto da Silva, L. Application of Engineered Nanomaterials as Nanocatalysts in Catalytic Ozonation: A Review. *Materials* **2024**, *17*, 3185. [CrossRef]
25. Zheng, T.-H.; Zhang, Z.-Z.; Liu, Y.; Zou, L.-H. Recent Progress in Catalytically Driven Advanced Oxidation Processes for Wastewater Treatment. *Catalysts* **2025**, *15*, 761. [CrossRef]
26. Broséus, R.; Vincent, S.; Aboulfadl, K.; Daneshvar, A.; Sauvé, S.; Barbeau, B.; Prévost, M. Ozone oxidation of pharmaceuticals, endocrine disruptors and pesticides during drinking water treatment. *Water Res.* **2009**, *43*, 4707–4717. [CrossRef]
27. Benner, J.; Salhi, E.; Ternes, T.; von Gunten, U. Ozonation of reverse osmosis concentrate: Kinetics and efficiency of beta blocker oxidation. *Water Res.* **2008**, *42*, 3003–3012. [CrossRef] [PubMed]
28. Ying, J.Y. Design and synthesis of nanostructured catalysts. *Chem. Eng. Sci.* **2006**, *61*, 1540–1548. [CrossRef]
29. Garcia-Ochoa, F.; Gomez, E. Bioreactor scale-up and oxygen transfer rate in microbial processes: An overview. *Biotechnol. Adv.* **2009**, *27*, 153–176. [CrossRef]
30. Bao, Y.; Jiang, Z.; Tong, S.; Huang, X.; Cai, Z.; Gao, Z. Reactive mass transfer of single O2 bubbles in a turbulent flow chamber. *Chem. Eng. Sci.* **2019**, *207*, 829–843. [CrossRef]
31. Petříček, R.; Moucha, T.; Rejl, F.J.; Valenz, L.; Haidl, J.; Čmelíková, T. Volumetric mass transfer coefficient, power input and gas hold-up in viscous liquid in mechanically agitated fermenters. Measurements and scale-up. *Int. J. Heat Mass Transf.* **2018**, *124*, 1117–1135. [CrossRef]
32. Villagómez-Cuéllar, M.A.; Bilbao-García, E.; Duoandicoechea, U.; Villota, N. Degradation of Carbamazepine by Ozonation: Influence of pH and Mass Transfer on Water Quality Improvement for Sustainable Water Treatment. *Sustainability* **2026**, *18*, 4246. [CrossRef]
33. Rivera-Utrilla, J.; López-Ramón, M.V.; Sánchez-Polo, M.; Álvarez, M.A.; Velo-Gala, I. Characteristics and Behavior of Different Catalysts Used for Water Decontamination in Photooxidation and Ozonation Processes. *Catalysts* **2020**, *10*, 1485. [CrossRef]
34. Rivas, F.J.; Beltrán, F.J.; Encinas, A. Removal of emergent contaminants: Integration of ozone and photocatalysis. *J. Environ. Manag.* **2012**, *100*, 10–15. [CrossRef] [PubMed]
35. Villota, N.; Ferreiro, C.; Qulatein, H.A.; Lomas, J.M.; Lombraña, J.I. Turbidity Changes during Carbamazepine Oxidation by Photo-Fenton. *Catalysts* **2021**, *11*, 894. [CrossRef]
36. Villota, N.; Ferreiro, C.; Qulatein, H.A.; Lomas, J.M.; Camarero, L.M.; Lombraña, J.I. Colour Changes during the Carbamazepine Oxidation by Photo-Fenton. *Catalysts* **2021**, *11*, 386. [CrossRef]
37. Liu, H.; Wang, C.; Wang, G. Photocatalytic Advanced Oxidation Processes for Water Treatment: Recent Advances and Perspective. *Chem. Asian J.* **2020**, *15*, 3239–3253. [CrossRef]
38. Schneider, J.; Matsuoka, M.; Takeuchi, M.; Zhang, J.; Horiuchi, Y.; Anpo, M.; Bahnemann, D.W. Understanding TiO_2 Photocatalysis: Mechanisms and Materials. *Chem. Rev.* **2014**, *114*, 9919–9986. [CrossRef]
39. Zhang, N.; Zhang, Y.; Xu, Y.-J. Recent progress on graphene-based photocatalysts: Current status and future perspectives. *Nanoscale* **2012**, *4*, 5792–5813. [CrossRef]
40. Low, J.; Yu, J.; Jaroniec, M.; Wageh, S.; Al-Ghamdi, A.A. Heterojunction photocatalysts. *Adv. Mater.* **2017**, *29*, 1601694. [CrossRef]
41. Fallah, N.; Bloise, E.; Santoro, D.; Mele, G. State of the Art and Perspectives in Catalytic Ozonation for Removal of Organic Pollutants in Water: Influence of Process and Operational Parameters. *Catalysts* **2023**, *13*, 324. [CrossRef]
42. Armaković, S.J.; Savanović, M.M.; Armaković, S. Titanium Dioxide as the Most Used Photocatalyst for Water Purification: An Overview. *Catalysts* **2023**, *13*, 26. [CrossRef]
43. *ISO 7027*; Water Quality—Determination of Turbidity. International Organization for Standardization (ISO): Geneva, Switzerland, 2016.